Reevaluation of Persistent Radical Effect in NMP

Wei Tang,[†] Takeshi Fukuda,*[,‡] and Krzysztof Matyjaszewski*[,†]

Center for Macromolecular Engineering, Department of Chemistry, Carnegie Mellon University, 4400 Fifth Avenue, Pittsburgh, Pennsylvania 15213, and Institute for Chemical Research, Kyoto University, Uji, Kyoto 611-0011, Japan

Received March 2, 2006; Revised Manuscript Received May 1, 2006

ABSTRACT: The persistent radical effect (PRE) originally proposed by H. Fischer was reevaluated. The original Fischer's equations for nitroxide-mediated polymerization (NMP) were examined, and new equations were derived to extend PRE treatment to higher conversions. The NMP kinetic process was divided into three stages, i.e., preequilibrium, transition period, and quasi-equilibrium, which were further analyzed separately. The kinetics for model reactions as well as for NMP of styrene and methyl methacrylate mediated by *N-tert*-butyl-*N*-[1-diethylphosphono-(2,2-dimethylpropyl)] nitroxide (also known as SG-1 or DEPN) were evaluated.

Introduction

Nitroxide-mediated polymerization (NMP) was the first successful controlled/living radical polymerization method (Scheme 1).[1,2] The persistent radical effect (PRE) for NMP, proposed originally by Fischer, described overall kinetics of NMP and also variation of concentration of growing (transient) and persistent (nitroxyl) radicals involved in NMP.[3−8] Equations derived for the concentrations of persistent and transient radicals predict a peculiar scaling with time$^{1/3}$ until a significant amount of persistent radical is formed. A similar treatment was proposed for the atom transfer radical polymerization (ATRP).[4] From such dependences the equilibrium constants in NMP and ATRP can be determined, provided that initial concentrations of all reagents and rate constant of termination (usually diffusion-controlled) were known (cf. eq 2). We recently reported that these equations cannot be applied for highly active ATRP systems when large amounts of persistent radicals are formed. Therefore, we derived new equations for ATRP, applicable from the time when the quasi-equilibrium between activation and deactivation is reached, to essentially infinite time.[9] These equations can be used for the precise determination of the equilibrium constants.

In this paper we extend the analysis to NMP systems and provide deeper insight into the operation of PRE by using Predici simulations.

Simulation. The Predici program (version 6.3.1) was used for kinetic modeling.[10,11] It employs an adaptive Rothe method as a numerical strategy for time discretization. Concentrations of all species can be followed. Calculations were performed on a personal computer and took approximately 3−5 min to complete.

Results and Discussion

Fischer's Equation. The persistent radical effect for nitroxide-mediated polymerization was originally described by Fischer.[3] In the absence of monomer (no propagation, k_p), the NMP equilibrium (Scheme 1) simplifies to three elementary reactions: activation (or dissociation of alkoxyamine R−Y, k_d), deactivation (or cross-coupling of transient radical R with persistent radical Y, k_c), and termination of transient radicals to form product P (k_t).

Scheme 1

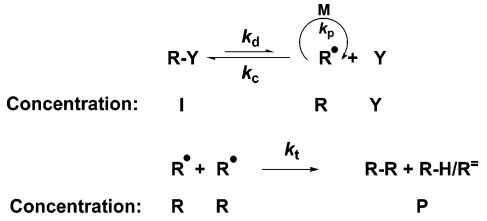

In this case, the rate of formation of the deactivator (the persistent radical, Y) and the rate of loss of the generated transient radical (R) are given by the following expressions (eq 1).

$$\frac{dR}{dt} = k_d I - k_c RY - 2k_t R^2$$

$$\frac{dY}{dt} = k_d I - k_c RY = \frac{dR}{dt} + 2k_t R^2 \qquad (1)$$

The term $2k_t$ is used in above expressions because a single termination step consumes two radicals. This is also in accordance with IUPAC's recommendation.[12]

The two coupled differential equations were solved analytically by Fischer[3,4,7,8] and also, independently, by Fukuda.[13,14] They proposed that the increase of concentration of deactivator (Y) should be proportional to $t^{1/3}$ and the loss of transient radical (R) proportional to $t^{-1/3}$ (eq 2).

$$Y = (6k_t K_{eq}^2 I_0^2)^{1/3} t^{1/3}$$

$$R = \left(\frac{K_{eq} I_0}{6k_t}\right)^{1/3} t^{-1/3} \qquad (2)$$

This dependence (for persistent radical, Y) should be valid in the time interval defined by eq 3. Equation 4 should be also fulfillled.[3,4,7,8]

$$t_L = \frac{4\sqrt{k_t} K_{eq}}{3 I_0^{1/2} k_d^{3/2}} < t < t_U = \frac{I_0}{48 K_{eq}^2 k_t} \qquad (3)$$

$$K_{eq} < I_0 k_c / 16 k_t \qquad (4)$$

[†] Carnegie Mellon University.
[‡] Kyoto University.
* Corresponding authors: e-mail km3b@andrew.cmu.edu, Fax 412-268-6897. E-mail: fukuda@scl.kyoto-u.ac.jp; fax: 81-774-38-3170.

10.1021/ma060465v CCC: $33.50
Published on Web 05/28/2006

Table 1. Rate Constants Used in the Simulations for SG-1-Based Nitroxide-Mediated Polymerization Systems

no.	M[a]	k_d (s^{-1})	k_c ($M^{-1}\,s^{-1}$)	K_{eq} (M)	k_t ($M^{-1}\,s^{-1}$)	k_p ($M^{-1}\,s^{-1}$)	temp (°C)	ref
1	(St)	0.01	5.0×10^5	2.0×10^{-8}	2.5×10^9	/	120	15, 16
2	St	0.011	5.5×10^5	2.0×10^{-8}	1.0×10^8	2.0×10^3	120	15, 16
3	MMA	0.01	1.4×10^4	7.1×10^{-7}	6.1×10^7	5.8×10^2	45	20

[a] St = Styrene; MMA = methyl methacrylate.

Scheme 2

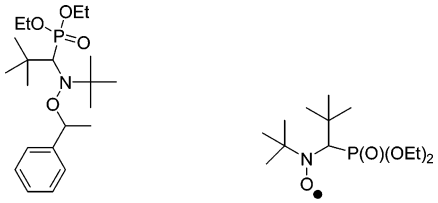

1-PhEt-SG1 SG1

All of the equations in this paper are slightly different from original Fischer's equations. For consistency, they were modified by replacing k_t with $2k_t$. Equation 4 was directly obtained by setting $t_L < t_U$, which differs from Fischer's original equation by a factor of 2.

Derivation of New Equations for PRE. The dependences described in eq 2, derived independently by Fischer and Fukuda,[4,13] used initial concentration of the initiator (I_0) rather than the actual one, I. However, in all radical systems, initiator concentration constantly decreases with the progress of the reaction. In our previous report, we proposed that it was more accurate to use the actual concentration of the initiator (and also catalyst in the ATRP system) to derive the kinetic equations for transient and persistent radicals, especially when reactions proceed to higher conversion.

A similar case is for NMP, although NMP equilibrium constants are relatively smaller than those in ATRP. Thus, a new equation for the evolution of persistent radical during the quasi-equilibrium stage was derived. The derivation is based on the stoichiometric requirement, i.e., $I_0 - I = Y$, and the assumption $dY/dt \gg -dR/dt$ after quasi-equilibrium (a detailed derivation is included in Appendix I).

The analytical solution of equations for NMP is similar to ATRP system. However, the solutions are different, since there is no catalyst (Cu^I species in ATRP) in NMP. Using variable I, the integration of eq 1 leads to the following expression

$$\frac{I_0^2}{I_0 - Y} + 2I_0 \ln \frac{I_0 - Y}{I_0} - (I_0 - Y) = 2k_t K_{eq}^2 t \qquad (5)$$

where the persistent radical concentration (Y) is the only variable on the left-hand side of the equation. Again, $2k_t$ was used in the derivation because two radicals were consumed in a single termination step. If one uses a new function $F(Y)$, where the only variable is Y

$$F(Y) = \frac{I_0^2}{I_0 - Y} + 2I_0 \ln \frac{I_0 - Y}{I_0} - (I_0 - Y) \qquad (6)$$

then a plot of $F(Y)$ vs t should provide a straight line with a slope $2k_tK_{eq}^2$. The equilibrium constants for NMP could be then calculated as $K_{eq} = \sqrt{\text{slope}/2k_t}$.

Model System 1-PhEt-SG1. Three NMP systems were studied using Predici simulations. They are based on *N-tert*-butyl-*N*-[1-diethylphosphono-(2,2-dimethylpropyl)] nitroxide (also known SG-1 or DEPN), as shown in Scheme 2. The corresponding alkoxyamines are quite labile and are characterized by large values of equilibrium constants, as shown in Table 1. We selected a model systems in polymerization of styrene without monomer (entry 1), the second one is styrene NMP, and the last one is NMP of methyl methacrylate. In the latter two cases the rate constants of dissociation and coupling for initiator and growing species are the same to simplify analysis. Indeed, the literature values for polystyrene and 1-PhEt-SG-1 are very similar.

Figure 1 compares, in double axes format, the plots for the

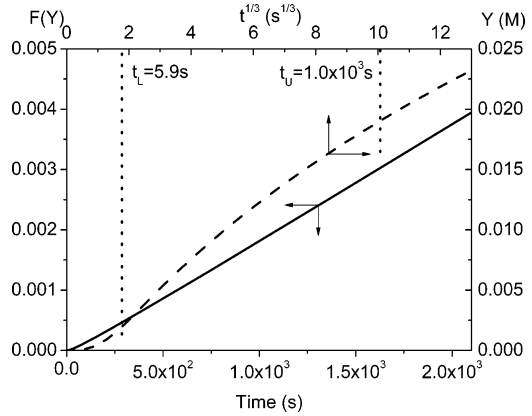

Figure 1. Kinetic data for persistent radical effect using new equation (—) and Fischer's equation (- - -); $k_d = 0.01\ s^{-1}$, $k_c = 5 \times 10^5\ M^{-1}\ s^{-1}$, $k_t = 2.5 \times 10^9\ M^{-1}\ s^{-1}$, $I_0 = 0.05$ M, K_{eq}(calc) $= 2.0 \times 10^{-8}$ M. $F(Y)$ is an expression as a function of Y (eq 6), and Y is the persistent radical concentration.

classic Fischer's equation (broken line showing Y vs $t^{1/3}$) and new equation (solid line depicting $F(Y)$ vs t) for a system with rate constants similar to those determined for 1-PhEt-SG1 (entry 1 in Table 1), a relatively active alkoxyamine at 120 °C.[15,16] Both plots should be linear. The plot based on the new eq 5 is perfectly straight and gives an equilibrium constant (2.0×10^{-8} M) identical to the actual one used in a kinetic simulation (2.0×10^{-8} M). However, the plot based on Fischer's eq 2 is not straight during the time range defined by eq 3, i.e., $1.8\ s^{1/3} < t^{1/3} < 10.1\ s^{1/3}$. The requirement (eq 4) proposed by Fischer for the validity of the eq 2 is obviously fulfilled for $k_c = 5.0 \times 10^5\ M^{-1}\ s^{-1}$ and $k_t = 2.5 \times 10^9\ M^{-1}\ s^{-1}$, i.e., $K_{eq} = 2.0 \times 10^{-8}\ M < I_0k_c/16k_t = 6.2 \times 10^{-7}$ M.[4,5]

The initial slope (5.9−100 s) from Fischer's plot gives $K_{eq} = 2.1 \times 10^{-8}$ M, the final slope (the last 10% before $t_U = 1.0 \times 10^3$ s) gives $K_{eq} = 0.85 \times 10^{-8}$ M, and the average value by fitting all data gives $K_{eq} = 1.4 \times 10^{-8}$ M.

Time Range Constraints. Although the time range defined by Fischer, when the dependence $Y \sim t^{1/3}$ should be valid (eqs 3 and 4), is fulfilled, deviations are observed.

If the upper time limit is inserted into eq 2, one obtains $Y/I_0 = 0.5$. This indicates that the buildup of persistent radical should reach 50% when the reaction time reaches the upper limit. This result contradicts Fischer's statement that there is "only very little conversion of R−Y to Y and P".[4] Even if one sets the upper time limit 10 times smaller, the R−Y conversion is still as high as 23.2%.

In fact, the persistent radical concentration is constantly increasing until it reaches I_0. There is a short stage when the

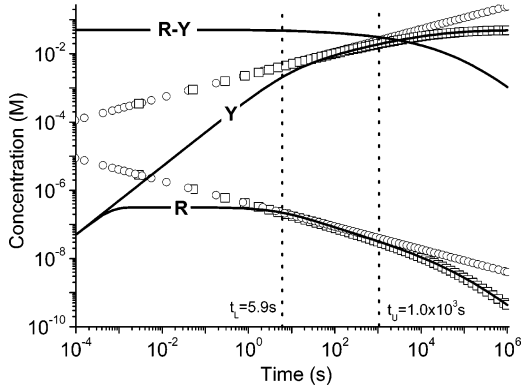

Figure 2. Evolution of concentrations of all species (solid lines) and concentrations of persistent radical predicted from new equation (□) and Fischer's equation (○); $k_d = 0.01\ s^{-1}$, $k_c = 5 \times 10^5\ M^{-1}\ s^{-1}$, $k_t = 2.5 \times 10^9\ M^{-1}\ s^{-1}$, $I_0 = 0.05$ M. K_{eq}(calc) $= 2.0 \times 10^{-8}$ M.

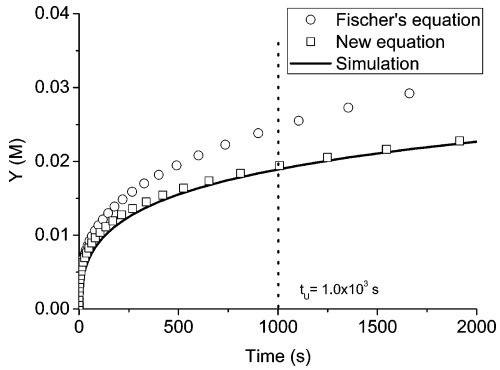

Figure 3. Simulated and calculated persistent radical values from new equation and Fischer's equation; $k_d = 0.01\ s^{-1}$, $k_c = 5 \times 10^5\ M^{-1}\ s^{-1}$, $k_t = 2.5 \times 10^9\ M^{-1}\ s^{-1}$, $I_0 = 0.05$ M. K_{eq}(calc) $= 1.0 \times 10^{-9}$ M. *Y* is the persistent radical concentration.

conversion of R−Y is very low, during which evolution of *Y* follows closely $t^{1/3}$, as predicted by Fischer's equation. This period corresponds to the linear part in the double-log plot of *Y* vs *t*, where the slope of this linear part is 1/3. However, the slope in the double-log plot is constantly changing due to progressive decrease of *I*. In fact, Fischer noticed a "deviation at long time" and stated that "these are noticeable although in the considerable time range the conversion is below 4%".[7]

Comparison of Original Fischer's and New Equations. To compare the new equations with Fischer's equations, the calculated values of *Y* from these two equations along with simulated one were plotted vs time in Figure 2. The data calculated from the new equation match perfectly with the simulation data after the system reaches quasi-equilibrium. The plot from Fischer's equation deviates slightly from simulated values in the indicated time range ($5.9\ s < t < 1.0 \times 10^3$ s). However, the deviation becomes much stronger in the linear time scale plot (Figure 3) because logarithmic plot decreases the difference. The difference increases with reaction time. At the point of upper time limit defined by Fischer, the deviation from the values predicted by the original equation is ∼31%.

As shown in Figure 2, Fischer's equation is valid only during a short period. This period (40−400 s) is much shorter than the time range proposed by Fischer ($5.9-1.0 \times 10^3$). The new equation does not have an upper time limit. The new equation is valid from the moment that system reaches quasi-equilibrium to essentially infinite time.

Analysis of PRE. Kinetic simulations help to better understand the evolution of all species in NMP and the dynamics of PRE. Figure 4 shows a double-axis plot for the evolution of concentrations of the initiator (*I*), the transient radical (*R*), and the persistent radical (*Y*) (solid green lines), as well as the activation rate (R_d), the deactivation rate (R_c), and the termination rate (R_t) (dotted thin black lines). Also, the dependences predicted from Fischer's equation (broken red lines) and from new equation (*Y* and *R*) (broken blue lines) are shown in Figure 4. The values of *R* (in blue) are calculated from the equilibrium equation (i.e., $R = K_{eq}I/Y$) using the values of *Y* from new equation. The whole process could be divided into three stages, i.e., preequilibrium, transition period, and quasi-equilibrium. These three stages will be analyzed separately.

Preequilibrium. When the reaction starts, concentrations of both *Y* and *R* increase linearly at the same rate. The *Y* and *R* are so small that the deactivation rate ($R_c = k_c RY$) is negligible

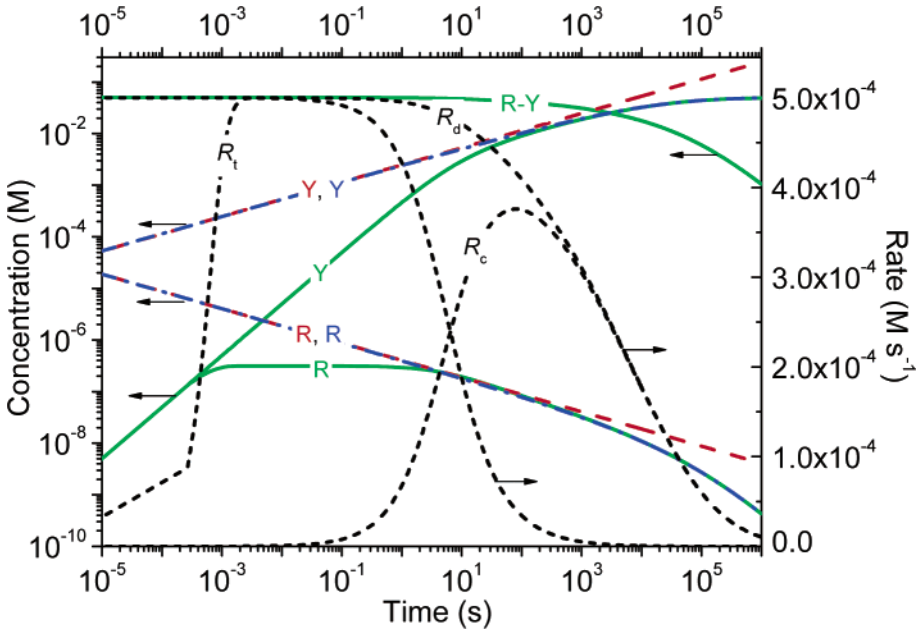

Figure 4. Simulated concentrations of all species (solid green lines) and concentrations predicted from new equation (broken blue line) and Fischer's equation (broken red line). Rates of activation (R_d), deactivation (R_c), and termination (R_t) shown as dotted black lines: $k_d = 0.01\ s^{-1}$, $k_c = 5 \times 10^5\ M^{-1}\ s^{-1}$, $k_t = 2.5 \times 10^9\ M^{-1}\ s^{-1}$, $I_0 = 0.05$ M. K_{eq}(calc) $= 2.0 \times 10^{-8}$ M.

Scheme 3

$$\text{R-Y} \xrightarrow{k_d} \text{R-R} + \text{Y}$$

compared to the activation rate ($R_d = k_d I$). The radicals are terminated by self-coupling with a rate $R_t = 2k_t R^2$, but the termination rate is also very small compared with R_d. Therefore, the reaction becomes a very simple one way reaction in the preequilibrium stage. For most cases during the preequilibrium, the change of initiator concentration is very small and can be neglected. So, $dR/dt = dY/dt = R_d = k_d I_0$, and after integration $R = Y = k_d I_0 t$.

The termination rate (R_t) increases faster than R_c due to the larger value of k_t (2.5×10^9 M^{-1} s^{-1}) than k_c (5×10^5 M^{-1} s^{-1}), although R and Y are almost the same during this period. Then R starts to deviate from the linear plot (Figure 4) due to self-termination, and this happens earlier than for Y. At this time, Y is still accumulating and follows the linear plot ($Y = k_d I_0 t$) because R_c is still very small as compared with R_d.

R reaches its maximum ($dR/dt = 0$, steady state) at the same moment when R_t reaches its maximum and becomes equal to R_d. This steady state holds for a short period during which decrease in R_t is balanced by increase in R_c.

The maximum value of R could be estimated as follows.

$$\frac{dY}{dt} = R_d = k_d I_0$$

$$\frac{dY}{dt} = \frac{dR}{dt} + 2k_t R^2 \approx 2k_t R^2 \qquad (7)$$

Thus, $k_d I_0 = 2k_t R^2$ and $R = \sqrt{k_d I_0 / 2k_t}$.

The start time when the transient radical reaches its steady state could be estimated by setting $R = k_d I_0 t = \sqrt{k_d I_0 / 2k_t}$, which gives $t_1 = 1/2k_d I_0 k_t$. The end time of this steady state could also be estimated by using Fischer's equation: $R = (K_{eq} I_0 / 6k_t)^{1/3} t^{-1/3} = \sqrt{k_d I_0 / 2k_t}$, which gives $t_2 = (\sqrt{8k_t} K_{eq})/6 I_0^{1/2} k_d^{3/2}$.

For larger equilibrium constant (K_{eq}), the steady state of the transient radical (R) is extended, and for deactivation negligibly slow, the system converts to a conventional radical polymerization.

During this period the accumulation of Y follows a simple exponential decay of I_0. Thus, $dY/dt = k_d I = k_d (I_0 - Y)$, and after integration, $Y = I_0(1 - e^{-k_d t})$. By following the evolution of Y (e.g., by EPR), the values of dissociation constant (k_d) could be obtained.

R starts to decrease and follow $t^{-1/3}$ behavior when R_c becomes larger than R_t. However, Y still increases linearly on the bilogarithmic plot. Then, when R_c increases to a sufficient level, evolution of Y changes from linear to $t^{1/3}$ according to the original Fischer's prediction.

Transition Period. During the transition period, the slope of the double-log plot for Y vs t will change from 1 to ~1/3 (eventually at the very long time will change to 0). The activation rate (R_d) is still almost constant. However, the deactivation rate (R_c) increases to reach the activation rate (R_d). The termination rate (R_t) becomes now smaller than deactivation rate (R_c) and continues to decrease due to the decrease of R. At this stage, the activation rate equals to the sum of the deactivation rate and termination rate, i.e., $R_d = R_c + R_t$. Also, $dY/dt = dR/dt + R_t \approx R_t$.

Thus, R starts to obey the $t^{-1/3}$ law when $R_c > R_t$, but Y obeys the $t^{1/3}$ law only when R_c approaches R_d and they reach quasi-equilibrium.

Quasi-Equilibrium. When R_d reaches the value of R_c, the system enters the third stage: quasi-equilibrium. During this stage, coupling is the major deactivation process, $R_c \gg R_t$. However, the progressive accumulation of the persistent radical Y also indicates the initiator concentration (I) is reduced to a significant extent. The activation rate (R_d) starts to decrease due to the significant consumption of initiator (this was not accounted for in the Fischer's treatment). The termination rate (R_t) continues to decrease to a very low level.

During this quasi-equilibrium stage, there is a short period where the slope of the double-log plot for Y vs t is ~1/3, i.e., $Y \sim t^{1/3}$. When the initiator concentration does not change much (<10%), the equations for the evolution of the persistent radical and transient radical are close to the power-law equations derived independently by Fischer and Fukuda.[4,13] The start point of this period (t_L) could be estimated when the two lines of $Y \sim t$ and $Y \sim t^{1/3}$ cross (as derived by Fischer), i.e.

$$Y = k_d I_0 t$$

$$Y = (6k_t K_{eq}^2 I_0^2)^{1/3} t^{1/3} \qquad (8)$$

So $t_L = (\sqrt{6k_t} K_{eq})/I_0^{1/2} k_d^{3/2}$, which is slightly larger than (1.84 times) the lower time limit derived by Fischer (eq 3). This also indicates that the quasi-equilibrium for persistent radical Y is reached later than for the transient radical R, as noticed but not explained by Fischer.[4]

As the equations above indicate (cf. also eq 3), the lower time limit (t_L) is determined by $K_{eq}/(I_0^{1/2} k_d^{3/2}) = k_d^{1/2} k_c / I_0^{1/2}$ ($k_t = 2.5 \times 10^9$ M^{-1} s^{-1} is assumed to be constant). The upper time limit (t_U) is determined by the initiator concentration and the equilibrium constant I_0/K_{eq}^2 (eq 3). Usually, the value of t_L is very small (several seconds); therefore, the length of time range for the validity of $Y \sim t^{1/3}$ is mostly determined by the equilibrium constant (I_0/K_{eq}^2).

When the conversion of Y is higher than 10%, larger deviations are expected for Fischer's equation with reaction time. However, the newly derived equation has no conversion limit and will match the simulation until essentially infinite time (Figure 2).

The Fischer's equations cannot be used for the precise determination of the equilibrium constants when a significant amount of persistent radical is formed. This is due to a constant curvature in Y vs $t^{1/3}$ (or R vs $t^{-1/3}$) coordinates. New equations give a linear dependence with a slope directly correlated with K_{eq}.

Polymerization of Styrene (St). According to Fischer and Fukuda, the evolution of monomer (M) should follow the equation[4,13]

$$\ln\left(\frac{M_0}{M}\right) = \frac{3}{2} k_p \left(\frac{K_{eq} I_0}{6k_t}\right)^{1/3} t^{2/3} \qquad (9)$$

Equation 9 was directly derived from eqs 2 which were based on the inaccurate assumption that the initiator concentration (R−Y or dormant species in polymerization) does not change during the reaction. Therefore, a new equation for monomer conversion was derived (details included in Appendix II).

$$\ln\left(\frac{M_0}{M}\right) = \frac{k_p}{2k_t K_{eq}} \left(I_0 \ln\left(\frac{I_0}{I_0 - Y}\right) - Y \right) \qquad (10)$$

To test Fischer's equation and new equation, the simulation for the polymerization of styrene was carried out by taking rate constants from literature (at 120 °C, entry 2 in Table 1), i.e., $k_d = 0.011$ s^{-1}, $k_c = 5.5 \times 10^5$ M^{-1} s^{-1}, $k_t = 1.0 \times 10^8$ M^{-1} s^{-1}, and $k_p = 2.0 \times 10^3$ M^{-1} s^{-1}.[15,16] The kinetic plots for monomer

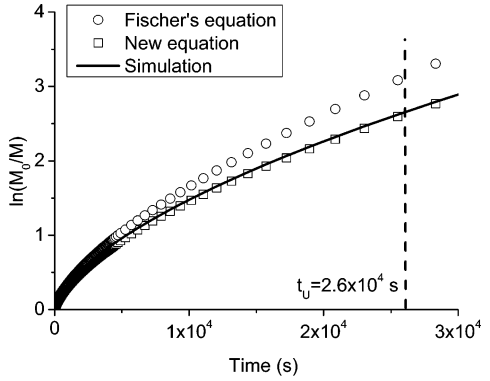

Figure 5. Semilogarithmic plots of monomer conversion for bulk polymerization of styrene: $k_d = 0.011\ s^{-1}$, $k_c = 5.5 \times 10^5\ M^{-1}\ s^{-1}$, $k_t = 1 \times 10^8\ M^{-1}\ s^{-1}$, $k_p = 2.0 \times 10^3\ M^{-1}\ s^{-1}$, $I_0 = 0.05$ M, $M_0 = 10$ M. $t_U = 2.6 \times 10^4$ s.

conversion from simulation and values calculated from Fischer's equation and the new equation are shown in Figure 5. The results from the newly derived equation perfectly match with those from simulation; however, the results from the Fischer's equation deviate at longer reaction times.

According to Fischer, the upper time limit (t_U) for the existence of $Y \sim t^{1/3}$ is 2.6×10^4 s (50% formation of Y). At this moment according to simulation and new equation, conversion of monomer is 92.7% but should be 95.4% according to Fischer's equation.

All the derivations of the kinetic equations were based on the constant value of termination rate constant (k_t), including the previous work of Fischer and Fukuda and this current work. However, chain-length-dependent termination can be further incorporated in the new model.[17−19] Thus, the model will become more complicated but more robust.

As we discussed in our previous paper, the equilibrium constants in ATRP can be determined from the $F(Y)$ vs t plot.[9] The concentration of Y (transition metal complex) can be easily followed by UV−vis spectroscopy. The same approach could be applied to determine the equilibrium constants in NMP by eq 5. However, the determination of Y for NMP usually requires ESR, which is not easily accessible. Another approach would be to determine the K_{eq} via the $\ln(M_0/M)$ vs t plot by coupling eq 5 and eq 10. Knowing k_p and k_t, one can determine K_{eq} by comparison of the experimental and theoretical rate curves (cf. Figure 5). One can find visually the best-fit value of K_{eq}, or (more preferably) one can use a least-squares program to fit kinetic data for various values of K_{eq}.

Polymerization of Methyl Methacrylate (MMA). With the new data available for the NMP of MMA by using a new SG1 initiator (Scheme 2),[20] Predici simulation was carried out for a simple reaction where $k_c = 1.4 \times 10^4\ M^{-1}\ s^{-1}$, $k_d = 1.0 \times 10^{-2}\ s^{-1}$, $k_t = 6.1 \times 10^7\ M^{-1}\ s^{-1}$, and $k_p = 5.8 \times 10^2\ M^{-1}\ s^{-1}$ (entry 3 in Table 1). However, these constants violate the kinetic requirement from Fischer (eq 4),[4] i.e., $K_{eq} = k_d/k_c = 7.14 \times 10^{-7}\ M > (I_0 k_c)/(16 k_t) = 1.8 \times 10^{-8}$ M.

As we can see from Figure 6, there is almost no quasi-equilibrium stage. Linear increase of Y directly goes directly into the end of reaction. Of course, there is also no match of Fischer's equation with simulation (Figure 6). In this case, the rate of termination (R_t) is almost the same as the rate of activation (R_d), which means most of the radicals are terminated once they are formed rather than deactivated by nitroxide. The period of steady state of radical is very long (10^{-3}−100 s); therefore, this reaction is more like a free radical polymerization process. Monomer consumption is slow during this stage. When

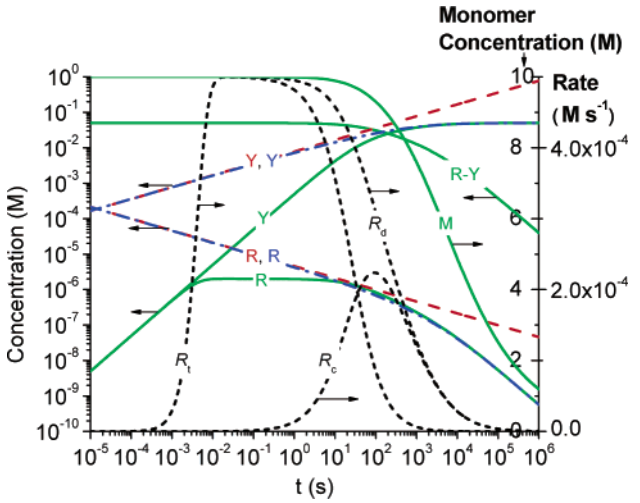

Figure 6. Simulation of a model NMP of MMA: concentrations of all species (solid green lines), concentrations predicted from new equation (broken blue line), and Fischer's equation (broken red line). Rates of activation (R_d), deactivation (R_c), and termination (R_t) are shown as broken black lines: $k_d = 0.01\ s^{-1}$, $k_c = 1.4 \times 10^4\ M^{-1}\ s^{-1}$, $k_t = 6.1 \times 10^7\ M^{-1}\ s^{-1}$, $I_0 = 0.05$ M. K_{eq}(calc) $= 7.14 \times 10^{-7}$ M, $M_0 = 10$ M.

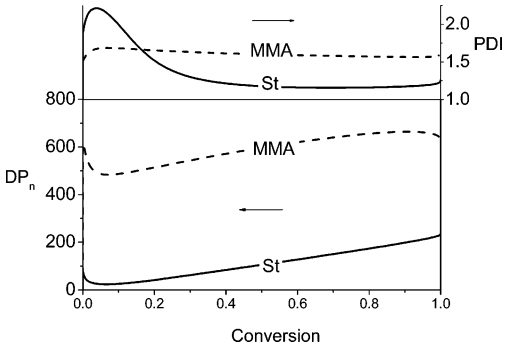

Figure 7. Simulation for the evolution of the number-average degree of polymerization (DP_n) and the polydispersity index ($PDI = M_w/M_n$) for NMP of St (entry 2 in Table 1) and MMA (entry 3 in Table 3). $I_0 = 0.05$ M, $M_0 = 10$ M, $DP_{th} = 200$.

monomer conversion reaches 42%, ∼90% of the dormant species are dead. No control is expected.

Figure 7 shows the evolution of the number-average degree of polymerization (DP_n) and polydispersity index ($PDI = M_w/M_n$) in polymerization of both St and MMA. NMP of St is well controlled and after a short initial period, DP linearly increases with monomer conversion and PDI decreases to ∼1.2. However, the NMP of MMA is not controlled. DP is much higher than theoretical one (200 at complete conversion), and PDI is also significantly higher than that for St.

Conclusions

The PRE equations originally derived by Fischer are not precise for systems when the amount of persistent radical produced exceeds ∼10%. They cannot provide correct K_{eq} values due to a constant curvature in $t^{1/3}$ dependence, since I_0 is constantly consumed. After equilibrium is established, the new equations are applicable up to very high conversion and essentially infinite reaction time.

Acknowledgment. The financial support from the National Science Foundation (CHE-04-05627) and CRP Consortium at CMU is gratefully acknowledged.

CDV

Appendix I. Derivation of New Equation for Persistent Radical

To derive the new equation, we follow the method of Fukuda et al.[13,21] The only difference is that Fukuda et al., as well as Fischer, discussed the case with $I = I_0$, while we remove this restriction so that $I = I_0 - Y$. The derivation of new equation is based on the kinetic expression (eq 1) and two assumptions. assumption 1 (equilibrium):

$$K_{eq} = \frac{RY}{I} \Rightarrow R = K_{eq}\frac{I_0 - Y}{Y} \tag{A1}$$

assumption 2:

$$\frac{dY}{dt} \gg -\frac{dR}{dt} \Rightarrow \frac{dY}{dt} \approx 2k_t R^2 \tag{A2}$$

Substituting assumption 1 into assumption 2, one obtains

$$\frac{Y^2}{(I_0 - Y)^2}\,dY = 2k_t K_{eq}{}^2\,dt \tag{A3}$$

After integration

$$\frac{I_0{}^2}{I_0 - Y} + 2I_0 \ln\left(\frac{I_0 - Y}{I_0}\right) - (I_0 - Y) = 2k_t K_{eq}{}^2 t \tag{A4}$$

Appendix II. Derivation of New Equation for Monomer Conversion

The rate of monomer consumption and the rate of accumulation of persistent radical follow the expression:

$$\frac{dM}{dt} = -k_p RM$$

$$\frac{dY}{dt} = \frac{dR}{dt} + 2k_t R^2 \approx 2k_t R^2 \tag{A5}$$

Dividing the first by the second expression gives

$$\frac{dM}{dY} = -\frac{k_p}{2k_t}\frac{M}{R} \tag{A6}$$

Since $R = K_{eq}I/Y = (K_{eq}(I_0 - Y))/Y$ (the equilibrium assumption), one gets

$$\frac{dM}{M} = -\frac{k_p}{2k_t K_{eq}}\frac{Y}{(I_0 - Y)}\,dY \tag{A7}$$

After integration, one obtains the kinetic equation for monomer

$$\ln\left(\frac{M_0}{M}\right) = \frac{k_p}{2k_t K_{eq}}\left(I_0 \ln\left(\frac{I_0}{I_0 - Y}\right) - Y\right) \tag{A8}$$

References and Notes

(1) Georges, M. K.; Veregin, R. P. N.; Kazmaier, P. M.; Hamer, G. K. *Macromolecules* **1993**, *26*, 2987−2988.
(2) Solomon, D. H.; Rizzardo, E.; Cacioli, P. U.S. Pat. 4581429*; Chem. Abstr*. **1985**, *102*, 221335q.
(3) Fischer, H. *Macromolecules* **1997**, *30*, 5666−5672.
(4) Fischer, H. *J. Polym. Sci., Part A: Polym. Chem.* **1999**, *37*, 1885−1901.
(5) Fischer, H. *Chem. Rev.* **2001**, *101*, 3581.
(6) Fischer, H.; Souaille, M. *Macromol. Symp.* **2001**, *174*, 231−240.
(7) Kothe, T.; Marque, S.; Martschke, R.; Popov, M.; Fischer, H. *J. Chem. Soc., Perkin Trans. 2* **1998**, 1553−1559.
(8) Souaille, M.; Fischer, H. *Macromolecules* **2000**, *33*, 7378−7394.
(9) Tang, W.; Tsarevsky, N. V.; Matyjaszewski, K. *J. Am. Chem. Soc.* **2006**, *128*, 1598−1604.
(10) Lutz, J.-F.; Matyjaszewski, K. *Macromol. Chem. Phys.* **2002**, *203*, 1385−1395.
(11) Wulkow, M. *Macromol. Theor. Simul.* **1996**, *5*, 393−416.
(12) Buback, M.; Egorov, M.; Gilbert, R. G.; Kaminsky, V.; Olaj, O. F.; Russell, G. T.; Vana, P.; Zifferer, G. *Macromol. Chem. Phys.* **2002**, *203*, 2570−2582.
(13) Ohno, K.; Tsujii, Y.; Miyamoto, T.; Fukuda, T.; Goto, M.; Kobayashi, K.; Akaike, T. *Macromolecules* **1998**, *31*, 1064−1069.
(14) Goto, A.; Fukuda, T. *Prog. Polym. Sci.* **2004**, *29*, 329−385.
(15) Benoit, D.; Grimaldi, S.; Robin, S.; Finet, J.-P.; Tordo, P.; Gnanou, Y. *J. Am. Chem. Soc.* **2000**, *122*, 5929−5939.
(16) Goto, A.; Fukuda, T. *Macromol. Chem. Phys.* **2000**, *201*, 2138−2142.
(17) Barner-Kowollik, C.; Buback, M.; Egorov, M.; Fukuda, T.; Goto, A.; Olaj, O. F.; Russell, G. T.; Vana, P.; Yamada, B.; Zetterlund, P. B. *Prog. Polym. Sci.* **2005**, *30*, 605−643.
(18) Shipp, D. A.; Matyjaszewski, K. *Macromolecules* **1999**, *32*, 2948−2955.
(19) Shipp, D. A.; Matyjaszewski, K. *Macromolecules* **2000**, *33*, 1553−1559.
(20) Guillaneuf, Y.; Gigmes, D.; Marque, S. R. A.; Bertin, D.; Tordo, P. *Macromol. Chem. Phys.* **2006**, in press.
(21) Fukuda, T.; Goto, A. *ACS Symp. Ser.* **2000**, *768*, 27.

MA060465V